Solvent-assisted linker exchange enabled preparation of cerium-based metal-organic frameworks constructed from redox active linkers

Journal:	*Inorganic Chemistry Frontiers*
Manuscript ID	QI-RES-09-2019-001218.R1
Article Type:	Research Article
Date Submitted by the Author:	24-Dec-2019
Complete List of Authors:	Son, Florencia; Northwestern University, Department of Chemistry Atilgan, Ahmet; Northwestern University, Department of Chemistry Idrees, Karam; Northwestern University, Department of Chemistry Islamoglu, Timur; Northwestern University, Department of Chemistry Farha, Omar; Northwestern University, Department of Chemistry

ARTICLE

Solvent-assisted linker exchange enabled preparation of cerium-based metal-organic frameworks constructed from redox active linkers

Received 00th January 20xx,
Accepted 00th January 20xx

DOI: 10.1039/x0xx00000x

Florencia A. Son,[a] Ahmet Atilgan,[a] Karam B. Idrees,[a] Timur Islamoglu,[a] and Omar K. Farha*[a,b]

Cerium based MOFs have shown much potential in fields such as catalysis and gas separation. However, hexanuclear Ce(IV) node MOFs are challenging to form in the presence of redox active species due to the ease of formation of Ce^{3+} in solution. Here, a facile solvent-assisted linker exchange procedure was developed to functionalize Ce-UiO-66 with amine and hydroxyl groups to produce MOFs that were unachievable *via de novo* methods. The resulting functionalized MOFs showed enhanced catalytic activity when testing the hydrolysis of the nerve agent simulant, dimethyl 4-nitrophenyl phosphate. By using an amine functionalized analogue of Ce-UiO-66, the hydrolysis rate was nearly doubled. With this study, we demonstrated that solvent-assisted linker exchange (SALE) is an effective tool to incorporate redox active linkers in Ce based MOFs that are otherwise unattainable *de novo*.

Introduction

Metal-organic frameworks (MOFs) are porous, crystalline materials composed of inorganic nodes and organic linkers[1] that have gained much interest due to their applications in gas separation processes,[2–5] gas storage,[6–8] and catalysis,[9,10] among many other fields. While their high degree of tunability makes them desirable materials due to the ability to target specific applications,[1] some MOFs are unattainable *via de novo* methods due to some thermodynamically favoured unwanted phases and/or functional group incompatibility which can lead to side reactions.[11–13]

In order to overcome these limitations, MOFs can undergo postsynthetic modifications (PSM).[14] More specifically, we can target a topology with a specific linker and node combination using a process called solvent-assisted linker exchange (SALE), also known as postsynthetic exchange,[15] where structural linkers in a pre-existing MOF can be replaced with a desired linker.[16–23] With SALE, we can not only synthesize MOFs that are inaccessible *de novo*, but we can also tune pore sizes[24,25] control catenation,[26,27] and alter their reactivities.[15,28,29] While SALE has been successfully performed on many MOFs, there is no procedure that can be used universally on cerium MOFs.

For this study, we focused on developing a SALE procedure for Ce-UiO-66, a Ce(IV) based UiO-66 analogue with the structural formula of $[Ce_6O_4(OH)_4(BDC)_6]$.[30,31] Like the zirconium analogue, the ideal structure of Ce-UiO-66 has hexanuclear clusters of $[Ce_6O_4(OH)_4]^{12+}$ that are connected by 12 dicarboxylate linkers.[30] Due to the high degree of connectivity,

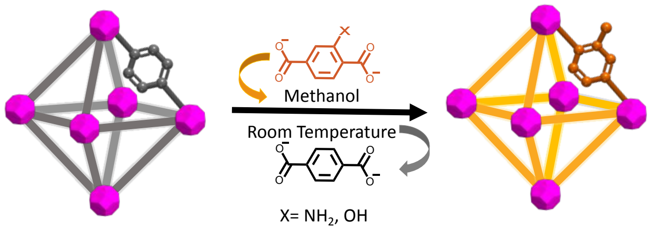

Figure 1. Depiction of SALE in Ce-UiO-66, where the pink polyhedra represent the metal nodes and the linkers are denoted by grey (parent) and orange (daughter).

UiO-66 and its analogues are able to withstand defects in the structure, such as missing linkers,[32–36] which aids in increasing the catalytic activity of the MOF.[37,38] Previously, our group has looked at utilizing Zr(IV) based MOFs for the detoxification of chemical warfare agents (CWAs) and later we reported that Ce(IV) analogues showed enhanced catalytic activity compared to Zr (IV) analogues.[31,39,40] The higher activity for the hydrolysis of organophosphate nerve agents of Ce(IV) compared to that of Zr(IV) has been credited to the presence of the 4f orbitals in Ce(IV), which allows for hybridization with the P=O bond's orbitals.[31] Additionally, we previously found that water binding is stronger in zirconium-based nodes than in cerium-based nodes, suggesting that there is an easier exchange of water on the cerium-based node with the substrate.[41] Due to the potential exhibited by Ce-UiO-66, we wanted to further enhance its catalytic activity through the functionalization of its linker by amino groups, which we showed its efficacy in zirconium-based MOFs.[42,43] However, the Ce MOFs of interest could not be synthesized *de novo*. Ce(IV) can easily be reduced during synthesis (Ce(III)/Ce(IV) of 1.61 V vs SHE),[44] which poses a challenge in synthesizing Ce (IV) MOFs with redox active linkers.[45]

Here, an effective SALE method (Figure 1) was investigated for the facile incorporation of the desired linkers into Ce-UiO-

---

[a] Department of Chemistry, International Institute of Nanotechnology,
[b] Department of Chemical and Biological Engineering, Northwestern University, 2145 Sheridan Road, Evanston, IL 60208, USA. Email: o-farha@northwestern.edu

†Electronic Supplementary Information (ESI) available: Materials, instrumentation, synthetic procedures of MOFs and DMNP, SEM images, ^{1}H NMR spectra, TGA curves. See DOI: 10.1039/x0xx00000x

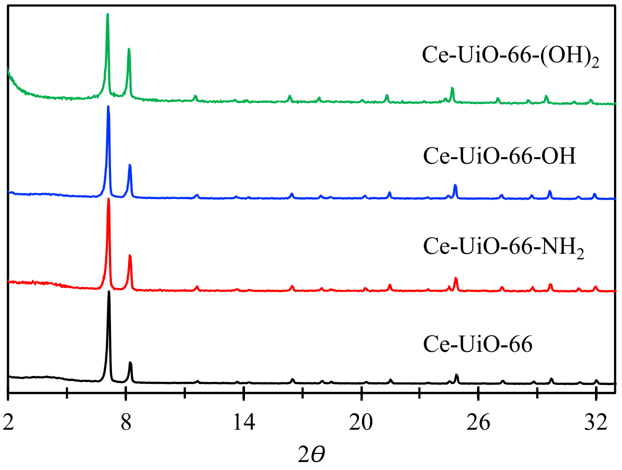

Figure 2. PXRD patterns of as-synthesized Ce-UiO-66 and SALE samples of Ce-UiO-66-NH$_2$, Ce-UiO-66-OH, and Ce-UiO-66-(OH)$_2$

66. Using methanol as our solvent,[46] we were able to successfully perform SALE on our solvothermally synthesized Ce-UiO-66 sample using 2-aminoterepthalic acid (BDC-NH$_2$), 2-hydroxyterephthalic acid (BDC-OH), as well as 2,5-dihydroxyterephthalic acid (BDC-(OH)$_2$). The hydrolysis experiments demonstrated that the functional groups were effective in enhancing the catalytic behavior of the parent Ce-UiO-66. Importantly, we were able to obtain three new MOFs that we could not obtain via solvothermal synthetic methods.

Experimental

Synthesis of Ce-UiO-66 [$Ce_6O_4(OH)_4(BDC)_6$]

Ce-UiO-66 was synthesized solvothermally using terephthalic acid (BDC) according to published procedures,[30,31] with a few alterations which can be found in the ESI.

Solvent-Assisted Linker Exchange (SALE) on Ce-UiO-66

In order to simplify calculations, we used the assumption that the formula of Ce-UiO-66 was that of a defect-free MOF. Ce-UiO-66 (0.1 mmol BDC), 2-aminoterephthalic acid (0.4 mmol), and 10 mL of methanol were vortexed to ensure dispersion in the solvent and then sonicated at room temperature for five minutes. The resulting MOF was washed three times with DMF to remove any excess linkers, washed three times with ethanol, and then soaked in ethanol overnight. The resulting powder was collected by centrifugation and dried in a vacuum oven at 80°C for half an hour to remove excess solvent. The powder product was transferred to a sample tube and then activated under vacuum at 40°C for 24 hours to remove any residual solvent molecules. To prevent any potential collapse due to thermal activation, lower temperatures were used. The same procedure was utilized for linker exchange with 2-hydroxyterephthalic acid and 2,5-dihydroxyterephtalic acid. We were able to successfully scale up the procedure. Further information can be found in the ESI.

Hydrolysis of dimethyl (4-nitrophenyl) phosphate (DMNP)

Ce-UiO-66 (1.5 µmol) was sonicated in 1 mL of a 10% D_2O solution (0.9 mL DI water/0.1 mL D_2O) for 10 seconds and 50 µL of the buffer ethyl morpholine (0.45 M) was subsequently added. The nerve agent simulant DMNP (25 µmol, Figure S6 and S7) was added and the mixture was shaken for 10 seconds and then transferred to an NMR tube. ^{31}P NMR spectra was collected in situ every minute for a total of 60 minutes.

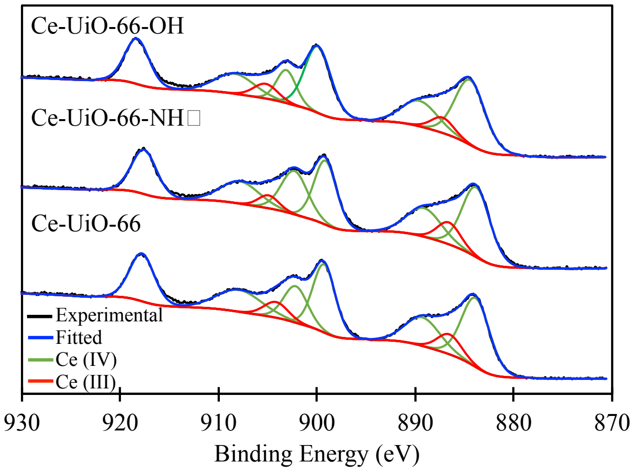

Figure 3. Experimental and fitted XPS spectra of Ce-UiO-66, Ce-UiO-66-NH$_2$, and Ce-UiO-66-OH corresponding to Ce 3d

Table 1. XPS data of Ce-UiO-66, Ce-UiO-66-NH$_2$, and Ce-UiO-66-OH

Sample	Binding Energy (eV)	Ce^{3+}
Ce-UiO-66	883.95	4.16%
Ce-UiO-66-NH$_2$	883.84	8.51%
Ce-UiO-66-OH	884.46	8.22%

Results and Discussion

SALE Characterization

As illustrated in Figure 2, we were able to confirm that the **fcu** topology and structural integrity in the SALE products were maintained by comparison of powder X-ray diffraction (PXRD) patterns before and after incorporation of the new linkers. Scanning electron microscopy (SEM) images showed that the overall particle morphology after SALE was not altered, indicating that the sonication method used for SALE was not harmful towards the crystals (Figure S1). X-ray photoelectron spectroscopy (XPS) revealed that the oxidation state of the MOFs after SALE predominantly remained at Ce(IV) (Figure 3). The electronic properties of the Ce MOFs were investigated by comparison of the binding energies. As anticipated, the more electron withdrawing groups yielded higher binding energies, while electron donating groups lowered the binding energies (Table 1).

Nitrogen isotherms that were collected at 77 K (Figure 4, top) showed Brunauer-Emmett-Teller (BET) surface areas of 1235 m^2/g for Ce-UiO-66, 1000 m^2/g for Ce-UiO-66-NH$_2$, and 1050 m^2/g for Ce-UiO-66-OH. Sorption data is not reported for Ce-UiO-66-(OH)$_2$ since we were unable to activate it thermally under vacuum and using supercritical CO_2. The pore size distribution analysis revealed the presence of defective sites, while maintaining similar pore sizes across all samples (Figure 4, bottom).

The success of the linker exchange was probed by looking at ^{1}H NMR spectra. Exchanges of 85±2%, 86±1%, and 85±2% were obtained when using BDC-NH$_2$, BDC-OH, and BDC-(OH)$_2$, respectively (Figure S5). Higher exchanges could be achieved with the BDC-NH$_2$ linker by repeating the SALE procedure twice;

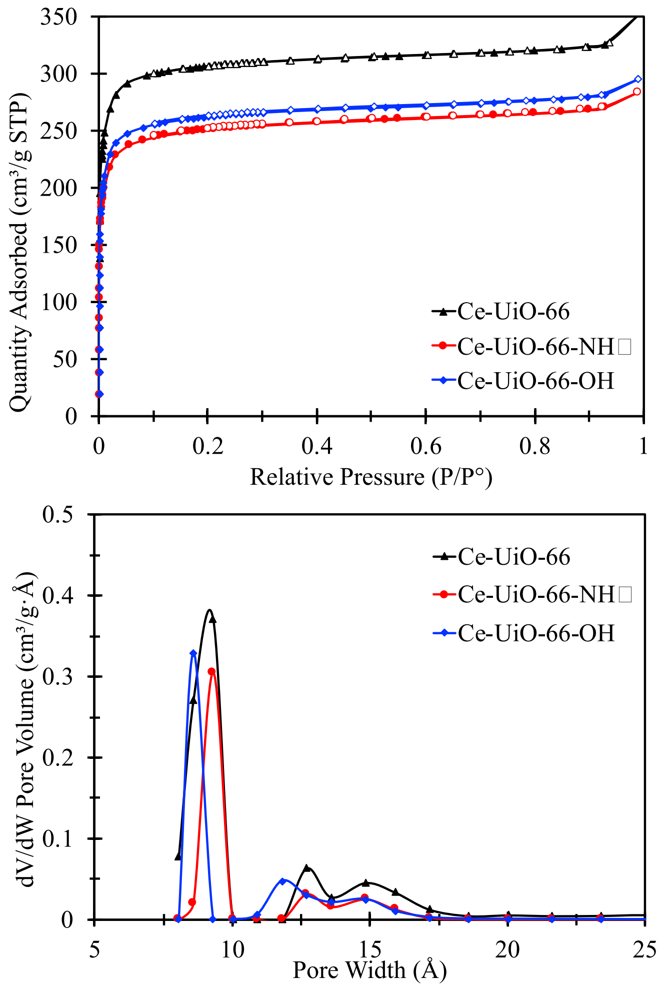

Figure 4. N_2 adsorption (closed markers) and desorption (open markers) at 77 K (top) and pore size distribution plots (bottom) for Ce-UiO-66, Ce-UiO-66-NH_2, and Ce-UiO-66-OH.

however, for the purpose of keeping comparable linker exchanges among all MOFs, we determined that the complete exchange was not necessary. The linker exchange rate was ascribed to the relatively weaker carboxylate-Ce coordination comparing to carboxylate-Zr coordination. When performing the same procedure on the zirconium analogue, UiO-66, less than 1% exchange with BDC-NH_2 was obtained.

We further investigated the effect of the functional group on the SALE process. Our experiments, in line with previous reports, showed that the pKa of the linker can impact the effectiveness of SALE.[29,43,47] Typically, carboxylic acids with higher pKa would result in stronger coordination with the Lewis acidic metal nodes. When using the procedure described above, but instead using equimolar amounts of both BDC-NH_2 and BDC-OH, the resulting MOF was found to contain 6% BDC, 30% BDC-NH_2, and 64% BDC-OH. Additionally, when performing SALE sequentially with first the amino functionalized linker and then followed by the hydroxyl functionalized linker, the final sample contained 3% BDC, 21% BDC-NH_2, and 76% BDC-OH.

Finally, based on thermogravimetric analysis results (Figures S2-S4), we were able to calculate the number of linkers per node for calculating the missing linker amounts. Ce-UiO-66 had 4.4 linkers per node, Ce-UiO-66-NH_2 had 4.5 linkers per node, and Ce-UiO-66-OH had 4.0 linkers per node, while a defect free sample would have 6 linkers per node. Surprisingly, performing SALE did not result in healing any present defects. Furthermore, additional defects were not generated, as was described to occur in Zr-UiO-66 when using methanol as the solvent which can imply the presence of missing cluster type defects.[46]

SALE Conditions

Prior to obtaining the SALE procedure described in the Experimental section, we tested and elucidated the impact of various factors such as solvent, time, temperature, and concentration.

To begin with, we first tested the effect of the solvent on the degree to which the linker exchange would occur. We started off by using methanol as our solvent system which was recently found to play a role in creating and stabilizing dangling linkers in the post-synthetic linker exchange of UiO-66.[46] These dangling linkers were found to behave similarly to monocarboxylate linkers and were able to undergo fast exchange.[46] Methanol was also found to be a highly efficient solvent for facilitating SALE in Ce-UiO-66 with the BDC derivatives. Furthermore, when comparing SALE with BDC-NH_2 in methanol versus in N,N-dimethylformamide (DMF) with a ratio of 2:1 of the daughter to the parent linker, we found that the exchange in methanol was 78% compared to 10% in DMF.

Due to SALE being an equilibrium process, we predicted that the equilibrium could be shifted to favor the incorporation of the daughter linker by having an excess of it present in solution. We began our studies by looking at a 2:1 daughter to parent linker ratio. Upon increasing the ratio to be 4:1 for BDC-NH_2, the exchange was increased from 78% to 85%.

Considering the time allowed for SALE to occur, we concluded that this was a fast equilibrium exchange process and that additional equilibration time was unnecessary. Many studies on other systems showed that a longer period of exchange time was necessary for the complete exchange with the desired linker. However, we found that in Ce-UiO-66 there was no enhancement in incorporation beyond the five-minute time frame. For example, with a 4:1 ratio of BDC-NH_2 to BDC with exchange times of 5 minutes, 30 minutes, and 2 hours, we found exchanges to be 85%, 84%, and 85%, respectively, which were highly comparable values.

Finally, we performed SALE at both room temperature and at 40°C where no enhancement was found in the exchange rate and/or extent. It is important to note that near complete SALE at room temperature could be beneficial for incorporating heat sensitive functional or protecting groups.

Hydrolysis of DMNP

The catalytic performance of MOFs for the degradation of the organophosphate nerve agents were previously shown to improve by using Ce(IV) over Zr(IV)[31] and additionally by incorporating amine functionality into the linkers.[48] We predicted that the combination of these characteristics would further improve the catalyst performance; however, a MOF

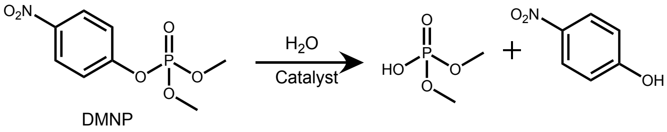

Scheme 1. Reaction scheme for hydrolysis of DMNP

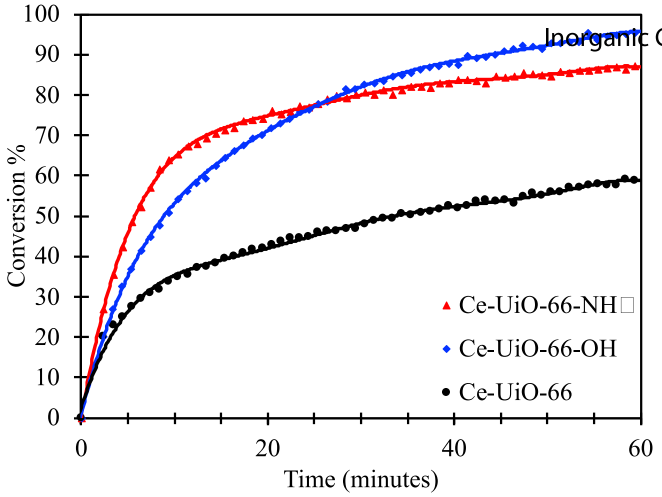

Figure 5. Conversion versus time for the hydrolysis of DMNP for Ce-UiO-66, Ce-UiO-66-NH_2, and Ce-UiO-66-OH.

combining the Ce precursor with the BDC-NH_2 linker could not be obtained without the use of SALE. We investigated the efficacy of our Ce MOFs obtained through SALE by looking at the hydrolysis of the nerve agent simulant dimethyl 4-nitrophenyl phosphate (DMNP) (Scheme 1). The heterogeneity of the catalyst system has been previously demonstrated in other studies.[30,31]

Table 2. Initial rates analysis for the hydrolysis of DMNP.

Sample	Rate constant	$t_{1/2}$
Ce-UiO-66	0.052±0.009	13.4±2.4
Ce-UiO-66-NH_2	0.112±0.005	6.2±0.3
Ce-UiO-66-OH	0.085±0.003	8.2±0.4

Using a catalyst loading of 6%, we monitored the conversion of DMNP over time (Figure 5 and S8), and the initial rates analysis (Table S1 and Figure S9) of Ce-UiO-66, Ce-UiO-66-OH, and Ce-UiO-66-NH_2 revealed half-lives of 13.4±2.4, 8.2±0.4, and 6.2±0.3 minutes (Table 2). With the UiO-66 system, pendant amines were determined to influence the microsolvation environment around the node, which helped lower the activation barrier for the rate determining step of the nucleophilic attack of water at the phosphorous center.[48] The improvement in the half-life of the amine functionalized Ce MOF compared to the parent MOF was observed, indicating that the amino group in the Ce analogue still manipulated the microsolvation around the node.

Beyond the functional group and electronic properties of the linker, the enhanced catalytic activity of the SALE samples was also attributed to the increase in the amount of Ce^{3+} present. As previously stated, there was a slight increase from 4.16% Ce^{3+} in Ce-UiO-66 to 8.51% for Ce-UiO-66-NH_2 and 8.22% for Ce-UiO-66-OH. The oxidation state of Ce has previously been demonstrated to influence it's catalytic behavior,[49–53] and work in our group has shown that increased Ce^{3+} character leads to enhanced DMNP hydrolysis,[54] which corroborates our observed results. The presence of Ce(III) has been proposed to enhance the catalytic activity due to the increased lability of water ligands on Ce(III) compared to Ce(IV), which can improve the hydrolysis of the simulant.[54,55] However, further work is needed to understand the role of Ce(III) in the catalytic degradation of organophosphate nerve agents.

Conclusions

In conclusion, we developed a methodology that allowed for the fast and efficient exchange of linkers for the introduction of functional groups within Ce-UiO-66 that were unattainable *de novo*. We demonstrated that this procedure was reproducible for several BDC derivatives.

We further demonstrated that this procedure allowed for altering the catalytic activity of the Ce-MOFs for the hydrolysis of the nerve agent simulant DMNP. The enhanced catalytic activity was found to be a result of not only the newly introduced functional groups, but also the oxidation state of the Ce node. The work presented represents a facile way to produce Ce MOFs that are unattainable *via de novo* methods.

Conflicts of interest

There are no conflicts to declare.

Acknowledgements

O.K.F. gratefully acknowledges support from the Defense Threat Reduction Agency (HDTRA1-19-1-0007 for the synthesis of MOFs and HDTRA1-18-1-0003 for catalysis work). This work made use of the IMSERC at Northwestern University, which has received support from the Soft and Hybrid Nanotechnology Experimental (SHyNE) Resource (NSF ECCS-1542205), the State of Illinois, and the International Institute for Nanotechnology (IIN). This work also made use of the Keck-II facility of Northwestern University's NU*ANCE* Center, which has received support from the Soft and Hybrid Nanotechnology Experimental (SHyNE) Resource (NSF ECCS-1542205); the MRSEC program (NSF DMR-1720139) at the Materials Research Center; the International Institute for Nanotechnology (IIN); the Keck Foundation; and the State of Illinois, through the IIN.

Notes and references

‡ Information regarding synthetic methods, instrumentation, as well as additional images and spectra can be found in the ESI.

1 H. Furukawa, K. E. Cordova, M. O'Keeffe and O. M. Yaghi, The chemistry and applications of metal-organic frameworks, *Science*, 2013, **341**, 974.

2 J.-R. Li, R. J. Kuppler and H.-C. Zhou, Selective gas adsorption and separation in metal–organic frameworks, *Chem. Soc. Rev.*, 2009, **38**, 1477–1504.

3 P. Nugent, Y. Belmabkhout, S. D. Burd, A. J. Cairns, R. Luebke, K. Forrest, T. Pham, S. Ma, B. Space, L. Wojtas, M. Eddaoudi and M. J. Zaworotko, Porous materials with optimal adsorption thermodynamics and kinetics for CO2 separation, *Nature*, 2013, **495**, 80–84.

4 R.-B. Lin, S. Xiang, H. Xing, W. Zhou and B. Chen, Exploration of porous metal–organic frameworks for gas separation and purification, *Coord. Chem. Rev.*, 2019, **378**, 87–103.

5 S. Kitagawa, Porous Materials and the Age of Gas, *Angew. Chemie Int. Ed.*, 2015, **54**, 10686–10687.

6 R. E. Morris and P. S. Wheatley, Gas Storage in Nanoporous Materials, *Angew. Chemie Int. Ed.*, 2008, **47**, 4966–4981.

7 Y. Peng, V. Krungleviciute, I. Eryazici, J. T. Hupp, O. K. Farha and T. Yildirim, Methane Storage in Metal–Organic Frameworks: Current Records, Surprise Findings, and

Challenges, *J. Am. Chem. Soc.*, 2013, **135**, 11887–11894.

8 J. L. C. Rowsell and O. M. Yaghi, Strategies for Hydrogen Storage in Metal-Organic Frameworks, *Angew. Chem. Int. Ed.*, 2005, **44**, 4670–4679.

9 J. Lee, O. K. Farha, J. Roberts, K. A. Scheidt, S. T. Nguyen and J. T. Hupp, Metal–organic framework materials as catalysts, *Chem. Soc. Rev.*, 2009, **38**, 1450–1459.

10 A. Fateeva, P. A. Chater, C. P. Ireland, A. A. Tahir, Y. Z. Khimyak, P. V. Wiper, J. R. Darwent and M. J. Rosseinsky, A Water-Stable Porphyrin-Based Metal-Organic Framework Active for Visible-Light Photocatalysis, *Angew. Chemie Int. Ed.*, 2012, **51**, 7440–7444.

11 O. Karagiaridi, W. Bury, J. E. Mondloch, J. T. Hupp and O. K. Farha, Solvent-Assisted Linker Exchange: An Alternative to the De Novo Synthesis of Unattainable Metal-Organic Frameworks, *Angew. Chemie Int. Ed.*, 2014, **53**, 4530–4540.

12 X. Gong, H. Noh, N. C. Gianneschi and O. K. Farha, Interrogating Kinetic versus Thermodynamic Topologies of Metal–Organic Frameworks via Combined Transmission Electron Microscopy and X-ray Diffraction Analysis, *J. Am. Chem. Soc.*, 2019, **141**, 6146–6151.

13 A. K. Cheetham, G. Kieslich and H. H.-M. Yeung, Thermodynamic and Kinetic Effects in the Crystallization of Metal–Organic Frameworks, *Acc. Chem. Res.*, 2018, **51**, 659–667.

14 Z. Wang and S. M. Cohen, Postsynthetic modification of metal–organic frameworks, *Chem. Soc. Rev.*, 2009, **38**, 1315–1329.

15 M. Kim, J. F. Cahill, Y. Su, K. A. Prather and S. M. Cohen, Postsynthetic ligand exchange as a route to functionalization of ‘inert’ metal–organic frameworks, *Chem. Sci.*, 2012, **3**, 126–130.

16 S. M. Cohen, Postsynthetic Methods for the Functionalization of Metal–Organic Frameworks, *Chem. Rev.*, 2012, **112**, 970–1000.

17 T. Islamoglu, S. Goswami, Z. Li, A. J. Howarth, O. K. Farha and J. T. Hupp, Postsynthetic Tuning of Metal-Organic Frameworks for Targeted Applications, *Acc. Chem. Res.*, 2017, **50**, 805–813.

18 P. Deria, J. E. Mondloch, O. Karagiaridi, W. Bury, J. T. Hupp and O. K. Farha, Beyond post-synthesis modification: evolution of metal-organic frameworks via building block replacement, *Chem. Soc. Rev*, 2014, **43**, 5896–5912.

19 B. J. Burnett, P. M. Barron, C. Hu and W. Choe, Stepwise Synthesis of Metal–Organic Frameworks: Replacement of Structural Organic Linkers, *J. Am. Chem. Soc.*, 2011, **133**, 9984–9987.

20 A. F. Gross, E. Sherman, S. L. Mahoney and J. J. Vajo, Reversible Ligand Exchange in a Metal–Organic Framework (MOF): Toward MOF-Based Dynamic Combinatorial Chemical Systems, *J. Phys. Chem. A*, 2013, **117**, 3771–3776.

21 K. Hirai, K. Chen, T. Fukushima, S. Horike, M. Kondo, N. Louvain, C. Kim, Y. Sakata, M. Meilikhov, O. Sakata, S. Kitagawa and S. Furukawa, Programmed crystallization via epitaxial growth and ligand replacement towards hybridizing porous coordination polymer crystals, *Dalt. Trans.*, 2013, **42**, 15868–15872.

22 S. Jeong, D. Kim, X. Song, M. Choi, N. Park and M. S. Lah, Postsynthetic Exchanges of the Pillaring Ligand in Three-Dimensional Metal–Organic Frameworks, *Chem. Mater.*, 2013, **25**, 1047–1054.

23 N. A. Vermeulen, O. Karagiaridi, A. A. Sarjeant, C. L. Stern, J. T. Hupp, O. K. Farha and J. F. Stoddart, Aromatizing Olefin Metathesis by Ligand Isolation inside a Metal–Organic Framework, *J. Am. Chem. Soc.*, 2013, **135**, 14916–14919.

24 O. Karagiaridi, W. Bury, E. Tylianakis, A. A. Sarjeant, J. T. Hupp and O. K. Farha, Opening Metal−Organic Frameworks Vol. 2: Inserting Longer Pillars into Pillared-Paddlewheel Structures through Solvent-Assisted Linker Exchange, *Chem. Mater.*, 2013, **25**, 3499–3503.

25 T. Li, M. T. Kozlowski, E. A. Doud, M. N. Blakely and N. L. Rosi, Stepwise Ligand Exchange for the Preparation of a Family of Mesoporous MOFs, *J. Am. Chem. Soc.*, 2013, **135**, 11688–11691.

26 T. Islamoglu, S. Goswami, Z. Li, A. J. Howarth, O. K. Farha and J. T. Hupp, Postsynthetic Tuning of Metal−Organic Frameworks for Targeted Applications, *Acc. Chem. Res*, 2017, **50**, 805–813.

27 W. Bury, D. Fairen-Jimenez, M. B. Lalonde, R. Q. Snurr, O. K. Farha and J. T. Hupp, Control over Catenation in Pillared Paddlewheel Metal–Organic Framework Materials via Solvent-Assisted Linker Exchange, *Chem. Mater.*, 2013, **25**, 739–744.

28 S. Takaishi, E. J. DeMarco, M. J. Pellin, O. K. Farha and J. T. Hupp, Solvent-assisted linker exchange (SALE) and post-assembly metallation in porphyrinic metal–organic framework materials, *Chem. Sci.*, 2013, **4**, 1509–1513.

29 O. Karagiaridi, M. B. Lalonde, W. Bury, A. A. Sarjeant, O. K. Farha and J. T. Hupp, Opening ZIF-8: A Catalytically Active Zeolitic Imidazolate Framework of Sodalite Topology with Unsubstituted Linkers, *J. Am. Chem. Soc.*, 2012, **134**, 18790–18796.

30 M. Lammert, M. T. Wharmby, S. Smolders, B. Bueken, A. Lieb, K. A. Lomachenko, D. De Vos and N. Stock, Cerium-based metal organic frameworks with UiO-66 architecture: Synthesis, properties and redox catalytic activity, *Chem. Commun.*, 2015, **51**, 12578–12581.

31 T. Islamoglu, A. Atilgan, S.-Y. Moon, G. W. Peterson, J. B. DeCoste, M. Hall, J. T. Hupp and O. K. Farha, Cerium(IV) vs Zirconium(IV) Based Metal–Organic Frameworks for Detoxification of a Nerve Agent, *Chem. Mater.*, 2017, **29**, 2672–2675.

32 M. J. Katz, Z. J. Brown, Y. J. Colón, P. W. Siu, K. A. Scheidt, R. Q. Snurr, J. T. Hupp and O. K. Farha, A facile synthesis of UiO-66, UiO-67 and their derivatives, *Chem. Commun.*, 2013, **49**, 9449–9451.

33 H. Wu, Y. Shen Chua, V. Krungleviciute, M. Tyagi, P. Chen, T. Yildirim and W. Zhou, Unusual and Highly Tunable Missing-Linker Defects in Zirconium Metal−Organic Framework UiO-66 and Their Important Effects on Gas Adsorption, *J. Am. Chem. Soc.*, 2013, 10525–10532.

34 M. R. DeStefano, T. Islamoglu, S. J. Garibay, J. T. Hupp and O. K. Farha, Room-Temperature Synthesis of UiO-66 and Thermal Modulation of Densities of Defect Sites, *Chem. Mater.*, 2017, **29**, 1357–1361.

35 R. J. Marshall and R. S. Forgan, Postsynthetic Modification of Zirconium Metal-Organic Frameworks, *Eur. J. Inorg. Chem.*, 2016, **2016**, 4310–4331.

36 Z. Hu, Y. Peng, Z. Kang, Y. Qian and D. Zhao, A Modulated Hydrothermal (MHT) Approach for the Facile Synthesis of UiO-66-Type MOFs, *Inorg. Chem.*, 2015, **54**, 4862–4868.

37 Y. Liu, R. C. Klet, J. T. Hupp and O. Farha, Probing the correlations between the defects in metal-organic frameworks and their catalytic activity by an epoxide ring-opening reaction, *Chem. Commun.*, 2016, **52**, 7806–7809.

38 F. Vermoortele, B. Bueken, G. Le Bars, B. Van de Voorde, M. Vandichel, K. Houthoofd, A. Vimont, M. Daturi, M.

Waroquier, V. Van Speybroeck, C. Kirschhock and D. E. De Vos, Synthesis Modulation as a Tool To Increase the Catalytic Activity of Metal–Organic Frameworks: The Unique Case of UiO-66(Zr), *J. Am. Chem. Soc.*, 2013, **135**, 11465–11468.

39 Y. Liu, A. J. Howarth, N. A. Vermeulen, S.-Y. Moon, J. T. Hupp and O. K. Farha, Catalytic degradation of chemical warfare agents and their simulants by metal-organic frameworks, *Coord. Chem. Rev.*, 2017, **346**, 101–111.

40 J. E. Mondloch, M. J. Katz, W. C. Isley III, P. Ghosh, P. Liao, W. Bury, G. W. Wagner, M. G. Hall, J. B. DeCoste, G. W. Peterson, R. Q. Snurr, C. J. Cramer, J. T. Hupp and O. K. Farha, Destruction of chemical warfare agents using metal-organic frameworks, *Nat. Mater.*, 2015, **14**, 512–516.

41 T. Islamoglu, D. Ray, P. Li, M. B. Majewski, I. Akpinar, X. Zhang, C. J. Cramer, L. Gagliardi and O. K. Farha, From Transition Metals to Lanthanides to Actinides: Metal-Mediated Tuning of Electronic Properties of Isostructural Metal–Organic Frameworks, *Inorg. Chem*, 2018, **57**, 13246–13251.

42 M. J. Katz, S.-Y. Moon, J. E. Mondloch, M. H. Beyzavi, C. J. Stephenson, J. T. Hupp and O. K. Farha, Exploiting parameter space in MOFs: a 20-fold enhancement of phosphate-ester hydrolysis with UiO-66-NH$_2$, *Chem. Sci.*, 2015, **6**, 2286–2291.

43 M. B. Lalonde, J. E. Mondloch, P. Deria, A. A. Sarjeant, S. S. Al-Juaid, O. I. Osman, O. K. Farha and J. T. Hupp, Selective Solvent-Assisted Linker Exchange (SALE) in a Series of Zeolitic Imidazolate Frameworks, *Inorg. Chem*, 2015, **54**, 7142–7144.

44 S. Smolders, A. Struyf, H. Reinsch, B. Bueken, T. Rhauderwiek, L. Mintrop, P. Kurz, N. Stock and D. E. De Vos, A precursor method for the synthesis of new Ce(IV) MOFs with reactive tetracarboxylate linkers, *Chem. Commun.*, 2018, **54**, 876–879.

45 T. Rhauderwiek, N. Heidenreich, H. Reinsch, S. Øien-Ødegaard, K. A. Lomachenko, U. Rütt, A. V. Soldatov, K. P. Lillerud and N. Stock, Co-Ligand Dependent Formation and Phase Transformation of Four Porphyrin-Based Cerium Metal–Organic Frameworks, *Cryst. Growth Des.*, 2017, **17**, 3462–3474.

46 J. Marreiros, C. Caratelli, J. Hajek, A. Krajnc, G. Fleury, B. Bueken, D. E. De Vos, G. Mali, M. B. J. Roeffaers, V. Van Speybroeck and R. Ameloot, Active Role of Methanol in Post-Synthetic Linker Exchange in the Metal-Organic Framework UiO-66, *Chem. Mater.*, 2019, **31**, 1359–1369.

47 O. Karagiaridi, W. Bury, A. A. Sarjeant, C. L. Stern, O. K. Farha and J. T. Hupp, Synthesis and characterization of isostructural cadmium zeolitic imidazolate frameworks via solvent-assisted linker exchange, *Chem. Sci.*, 2012, **3**, 3256–3260.

48 T. Islamoglu, M. A. Ortuño, E. Proussaloglou, A. J. Howarth, N. A. Vermeulen, A. Atilgan, A. M. Asiri, C. J. Cramer and O. K. Farha, Presence versus Proximity: The Role of Pendant Amines in the Catalytic Hydrolysis of a Nerve Agent Simulant, *Angew. Chemie - Int. Ed.*, 2018, **57**, 1949–1953.

49 S. Smolders, K. A. Lomachenko, B. Bueken, A. Struyf, A. L. Bugaev, C. Atzori, N. Stock, C. Lamberti, M. B. J. Roeffaers and D. E. De Vos, Unravelling the Redox-catalytic Behavior of Ce^{4+} Metal-Organic Frameworks by X-ray Absorption Spectroscopy, *ChemPhysChem*, 2018, **19**, 373–378.

50 N. Heidenreich, S. Waitschat and H. Reinsch, Investigation of the Kinetic Stabilization of a Ce^{4+}-based MOF by in-situ Powder X-ray Diffraction, *Zeitschrift für Anorg. und Allg. Chemie*, 2018, **644**, 1826–1831.

51 L. Luo, L. Huang, X. Liu, W. Zhang, X. Yao, L. Dou, X. Zhang, Y. Nian, J. Sun and J. Wang, Mixed-Valence Ce-BPyDC Metal–Organic Framework with Dual Enzyme-like Activities for Colorimetric Biosensing, *Inorg. Chem.*, 2019, **58**, 11382–11388.

52 M. Y. Masoomi, A. Morsali, A. Dhakshinamoorthy and H. Garcia, Mixed-Metal MOFs: Unique Opportunities in Metal-Organic Framework (MOF) Functionality and Design, *Angew. Chemie Int. Ed.*, 2019, **58**, 2–20.

53 Y. Xiong, S. Chen, F. Ye, L. Su, C. Zhang, S. Shen and S. Zhao, Synthesis of a mixed valence state Ce-MOF as an oxidase mimetic for the colorimetric detection of biothiols, *Chem. Commun.*, 2015, **51**, 4635–4638.

54 J. Liu, L. R. Redfern, Y. Liao, T. Islamoglu, A. Atilgan, O. K. Farha and J. T. Hupp, Metal–Organic-Framework-Supported and -Isolated Ceria Clusters with Mixed Oxidation States, *ACS Appl. Mater. Interfaces*, 2019, DOI:10.1021/acsami.9b12261.

55 M. R. Momeni and C. J. Cramer, Dual Role of Water in Heterogeneous Catalytic Hydrolysis of Sarin by Zirconium-Based Metal–Organic Frameworks, *ACS Appl. Mater. Interfaces*, 2018, **10**, 18435–18439.